Strain Rate Concentration Factor for Double-Edge-Notched Specimens Subjected to High Speed Tensile Loads

Nao-Aki NODA[1,*], Yoshikazu SANO[1], Makoto ANDO[1], Yoshihito KUROSHIMA[1], Takahiro SHINOZAKI[1], Hayato OHTSUKA[1] and Wenhai GUAN[1]

[1] Department of Mechanical and Control Engineering, Kyushu Institute of Technology,
1-1 Sensui-cho, Tobata-ku, Kitakyushu-city, Fukuoka, 804-8550, Japan
* Corresponding author: noda@mech.kyutech.ac.jp

Abstract Engineering plastics provide superior performance to ordinary plastics for wide range of the use. For polymer materials, dynamic stress and strain rate may be major factors to be considered when the strength is evaluated. Recently, high speed tensile test is being recognized as a standard testing method to confirm the strength under dynamic loads. In this study, therefore, high speed tensile test is analyzed by the finite element method; then, the maximum dynamic stress and strain rate are discussed with varying the tensile speed and maximum forced displacement. The strain rate concentration factor found to be constant independent of tensile speed, which is defined $K_{t\dot{\varepsilon}}$ as the maximum strain rate appeared at the notch root over the average nominal strain rate at the minimum section. The maximum strain rate is controlled by the tensile speed alone independent of the magnitude of the forced displacement. It is found that the difference between static and dynamic maximum stress concentration (σ_{max}-σ_{st}) at the notch root is proportional to the tensile speed when u/t$\leqq$5000mm/s.

Keywords Stress Concentration, Notch, Dynamic Stress, Strain Rate, Finite Element Method

1. Introduction

Engineering plastics are widely used in everyday products. Typically, a suitable engineering plastic is chosen for its range of enhanced physical properties. It is know that polycarbonate has superior impact and perforation resistance compared with other polymers, or indeed compared with some structural metals [1]. Most thermoplastics far below their glass transition temperature T_g give a brittle fracture when deformed in uniaxial tension. However, polycarbonate is an exception and deformed in a ductile manner. However, Izod impact studies of notched specimens show that the fracture mode changes from ductile to brittle below T_g. To investigate the brittle-ductile transition, which is affected by temperature and loading speed [2, 3], a high-speed tensile test is being recognized as a standard testing method in recent years. Generally, bluntly notched specimens failed in a fully ductile manner, and sharply notched specimens failed in brittle manner depending on the strain rate at the notch root.

It should be noted that Izod and Charpy impact tests are not suitable for evaluating the impact strength of real products because the impact speeds do not correspond to the real failure. In the high-speed tensile test, it is necessary to obtain the strain rate correctly to understand the impact strength of the polymer specimen. For smoothing specimens, the strain rate can be determined as $\dot{\varepsilon} = u/tl$ from the specimen length l and the tensile speed u/t. On the other hand, for notched specimens, it is necessary to measure the strain at the notch root by strain gauge measurement, for example. However, because only the average value of the strain concerning the gauge width can be measured. It is not easy to measure the strain at the notch root.

In the previous studies for dynamic stress concentration, circular holes [4] and elliptical holes [5] were investigated under step load [6, 7] and pulse load [7, 8]. In addition, several review papers for

impact problems are also available [9–11]. However, there are few studies on the strain rate concentration for notched specimens under various tensile speed. Therefore, in this paper, the finite element method is applied to analyze the notched specimens under various tensile speed. Then, the dynamic stress concentration factor and the strain rate factor will be discussed with varying tensile speed and maximum values of forced displacement.

2. Static stress concentration and specimen geometry

In this study, the material analyzed is assumed as polycarbonate, which has especially high impact strength among the polymeric materials. Young's modulus is assumed as E = 2.3GPa, Poisson's ratio ν = 0.37. Figure 1 shows the geometry of the double-edge-notched specimen, with dimensions of notch root radius $\rho = 0.03mm$ and $0.2mm$, notch depth t = 5mm, and opening angle 90º. The notch root radius $\rho = 0.03mm$ corresponds to the radius of fillet appearing at polymer products generally. The notch root radius $\rho = 0.2mm$ corresponds to the radius of the notched specimens used in the Izod and Charpy test. When the high-speed tensile test is performed, both ends of the specimen are gripped by rigid chuck, then forced displacement is applied to the end under constant speed. Figure 2 shows FE models for analysis. Here Model 1 has the notch radius $\rho = 0.03mm$, and Model 2 has $\rho = 0.2mm$. Figure 2(c) shows the notch root detail in Model 1, and Fig. 2(d) shows the notch root detail in Model 2. Minimum mesh size of the notch root is $e = \rho/243$ each model. Figure 3 shows the boundary conditions given to the end portion of the analysis models. Figure 3(a) shows boundary conditions in the rigid chucks, and Fig.3(b) shows a tensile stress boundary conditions

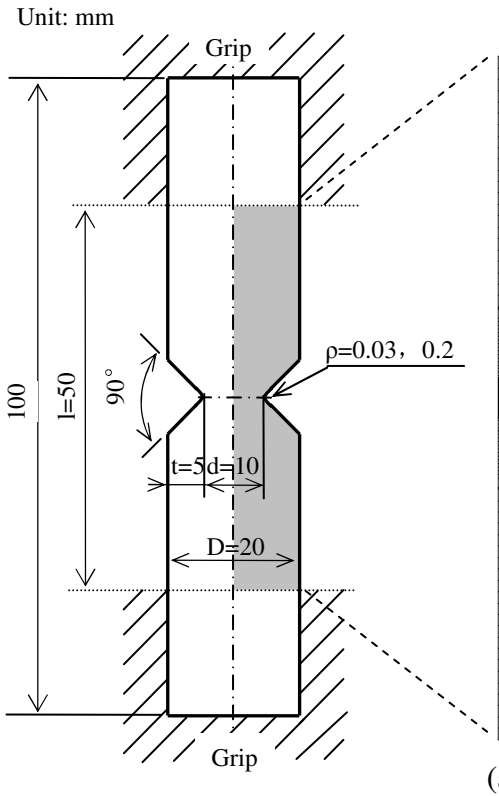

Figure 1. Geometry of specimen

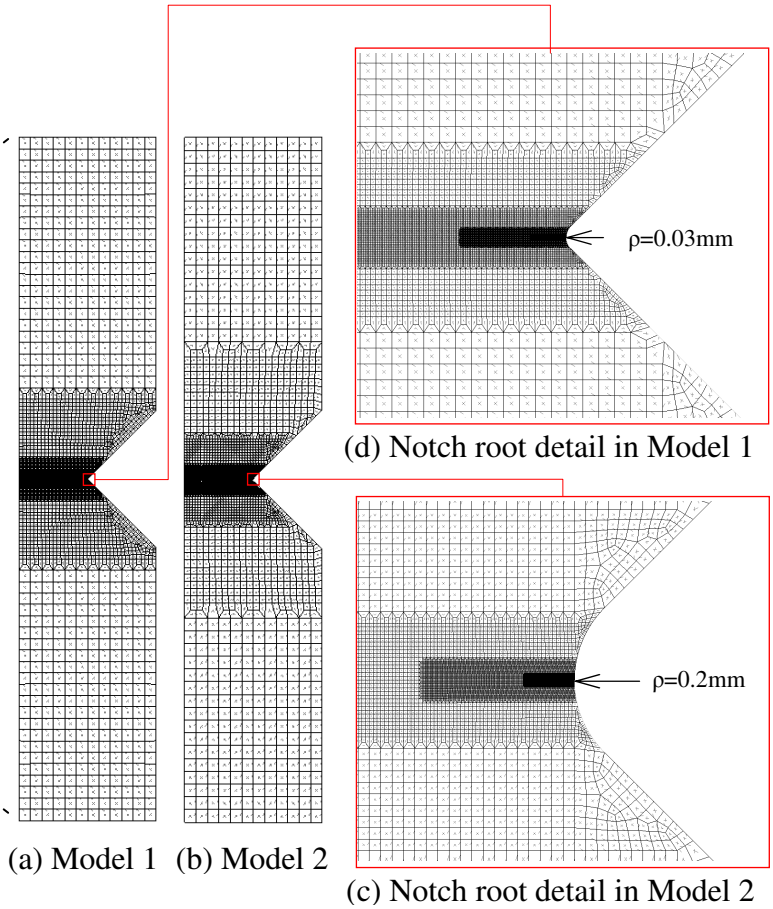

Figure 2. FE models

generally used. Table 1 shows the effect of boundary conditions on the static stress concentration factor. From Table 1, it is seen that the stress concentration factor is almost the same between the rigid grip tension and simple tension. Also, Table 1 shows the FE model in Fig. 2 shows less than 1% error compared to the exact stress concentration factor obtained by the approximate formula[12].

3. Dynamic stress concentration for high speed tensile test specimen

Figure 4 shows the forced displacement u given at the end of the specimen. The average stress σ_{gross} is also indicated, which is expressed as $\sigma_{gross}(t) = 0.867E \cdot u(t)/l$ from FEM. The stress at the

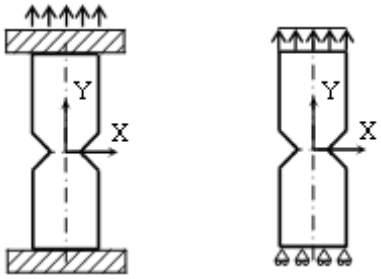

(a)Rigid grip tension (b)Simple tension

Figure 3. Boundary condition

Table 1. Static stress concentration factor by FEM

	K_t in Fig.3(a)	K_t in Fig.3(b)	Ref. [12] in Fig.3(b)
ρ=0.03, t=5	14.46	14.48	14.49
ρ=0.2, t=5	6.14	6.15	6.12

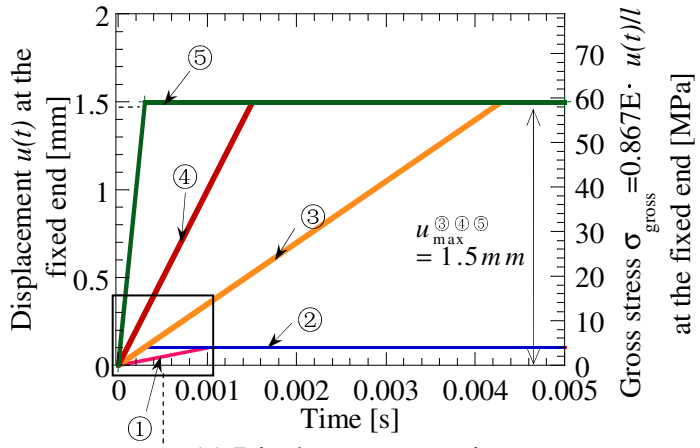

(a) Displacement vs. time

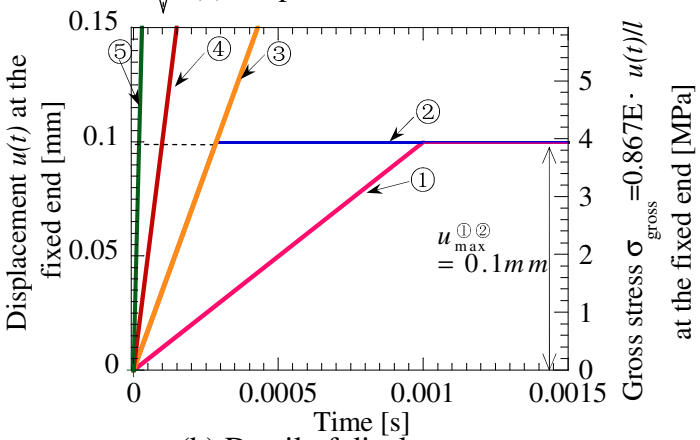

(b) Detail of displacement

Figure 4. Loading conditions

minimum section is expressed as $\sigma_{net} = (D/d)\sigma_{gross}$. Here, we consider 5 cases as shown in Table 2. Table 2 shows the tensile speed and the maximum forced displacement at the grip end with the time of that appear. In Case 5, the tensile speed $u/t = 5000\,mm/s$ corresponds to the impact speed when someone drops a call phone to the ground. The maximum displacement 1.5mm corresponds to the brittle fracture appears for high speed tensile test. The maximum displacement 0.1mm corresponds to an example of nondestructive case of for high speed tensile test.

Figure 5 shows the dynamic stress at the notch root A for Cases 1-5. Also Fig. 5 shows the detail of the dynamic stress oscillation with each case. From Fig. 4 and Fig. 5, it is seen that the maximum dynamic stress $\sigma_{\max}$ appears at almost the same time of the maximum forced displacement. Defined the maximum value of dynamic stress as $\sigma_{\max}$ in each case. After several oscillations due

Table 2. Maximum displacement and tensile speed given at the grip end

	Case		①	②	③	④	⑤
Condition	Maximum displacement	$u_{\max}$	0.1 mm t=0.00100s	0.1 mm t=0.00029s	1.5 mm t=0.00429s	1.5 mm t=0.00150s	1.5 mm t=0.00030s
	Tensile speed	u/t	100 mm/s t<0.00100s	350 mm/s t<0.00029s	350 mm/s t<0.00429s	1000 mm/s t<0.00150s	5000 mm/s t<0.00030s

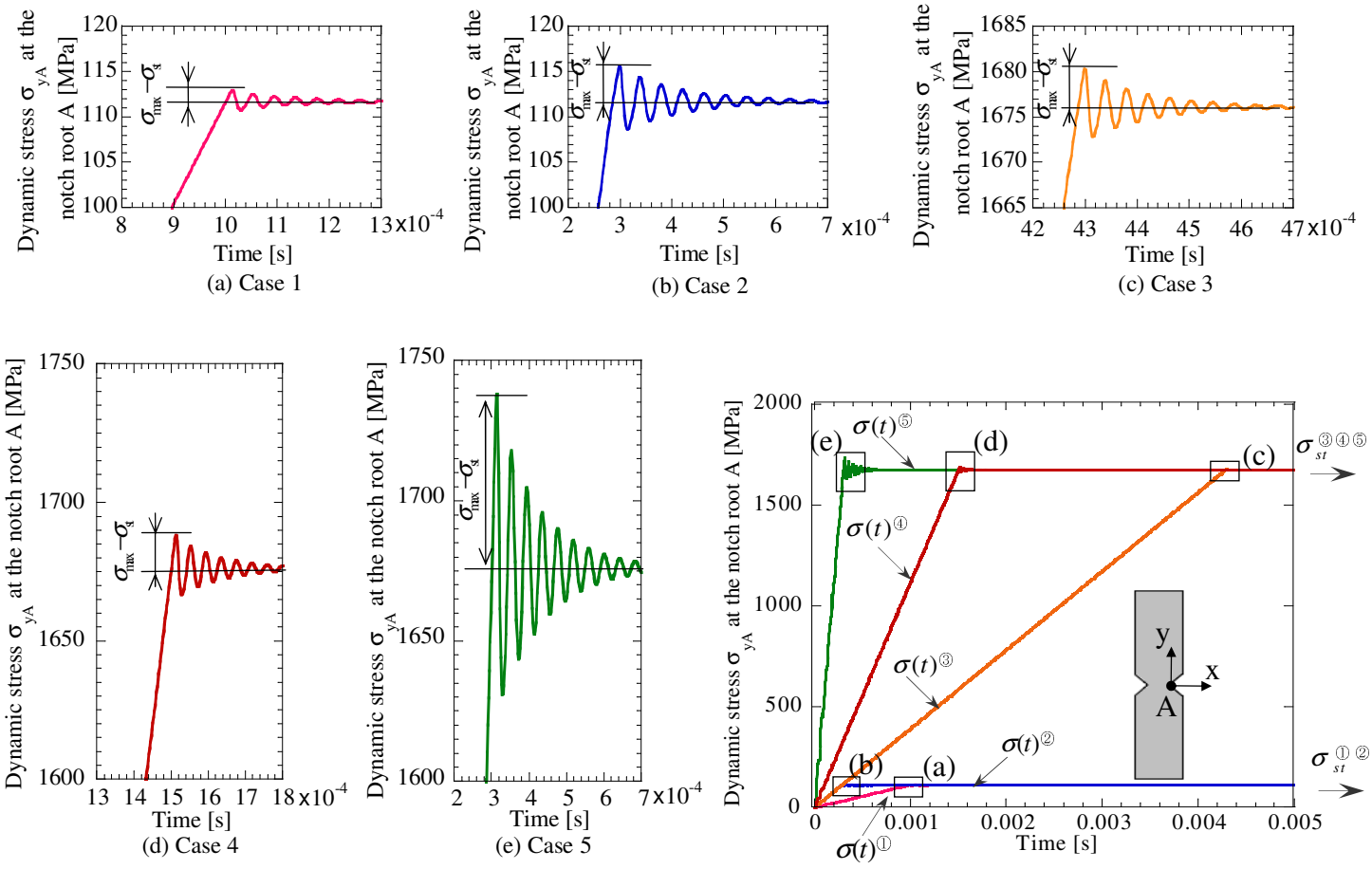

Figure 5. Dynamic stress at notch root A for ρ=0.03mm

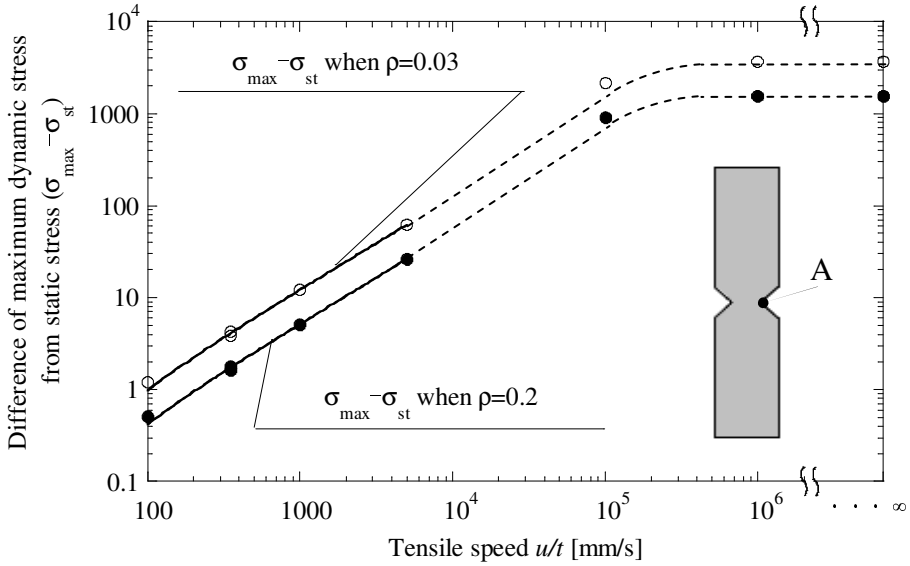

Figure 6. Difference between the static and dynamic maximum stress concentration ($\sigma_{\max} - \sigma_{st}$) vs. tensile speed

to the stress wave, dynamic stress approaches the static stress σ_{st}. From the comparison between Case 3 and Case 4, it is seen that of the maximum dynamic stress oscillation $(\sigma_{\max} - \sigma_{st})$ at the notch root A is always the same although the final displacement of Case 3 is 15 times larger than that in Case 2. It is may be concluded that the maximum dynamic stress oscillation $(\sigma_{\max} - \sigma_{st})$ is controlled by the tensile speed. Figure 6 shows the relationship between the tensile speed u/t and $(\sigma_{\max} - \sigma_{st})$ for $\rho = 0.03mm$ and $0.2mm$. Here the results for $u/t = 10^5, 10^6\, mm/s$ and step load $u/t = \infty$ are also indicated when the maximum displacement is 1.5mm. It is seen that $(\sigma_{\max} - \sigma_{st})$ is proportional to the tensile speed when $u/t \le 5000\, mm/s$. However, $(\sigma_{\max} - \sigma_{st})$ becomes constant when $u/t \ge 10^5\, mm/s$.

4. Strain rate concentration for high speed tensile test specimen

Figure 7 shows the strain rate at the notch root A for Cases 1-5. The strain rate increases dramatically at the start of applying forced displacement, Then, after several oscillations, the strain

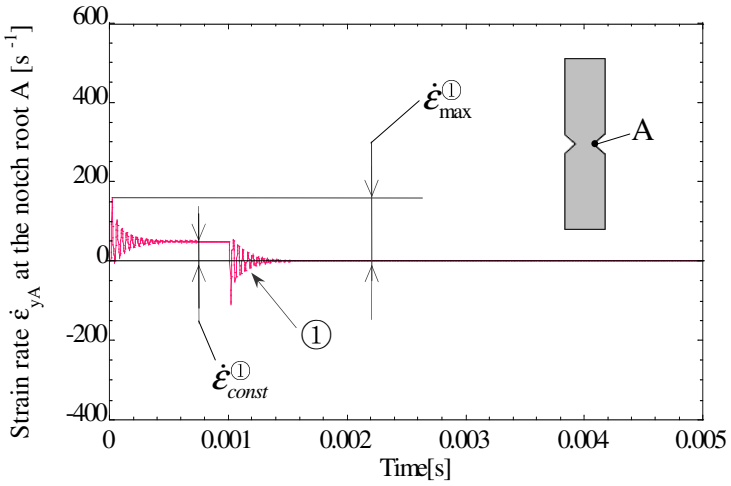

(a) Case 1

Figure 7. Strain rate at notch root A for ρ=0.03mm (Continued on next page)

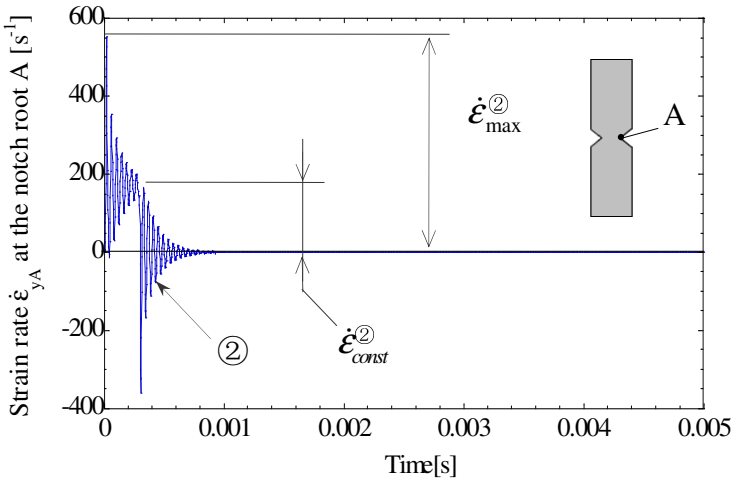

(b) Case 2

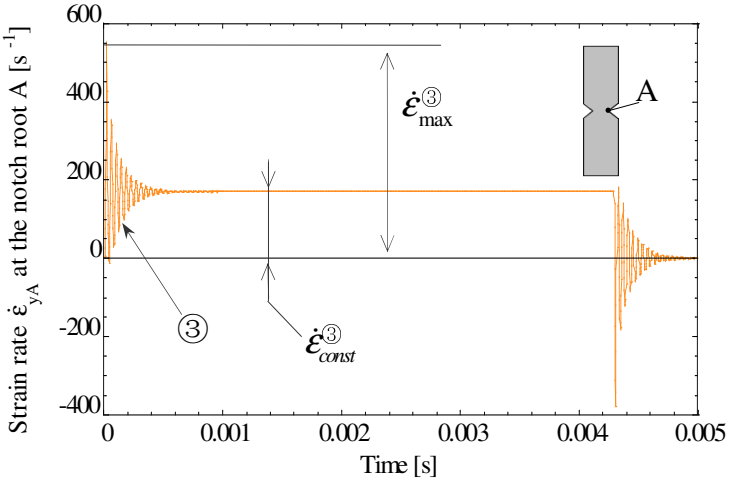

(c) Case 3

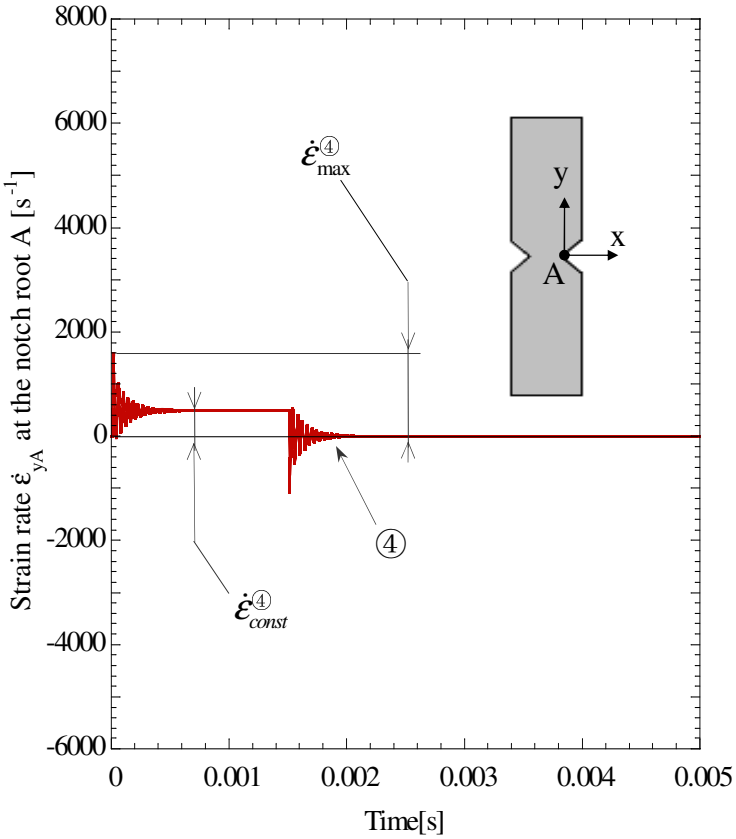

(d) Case 4

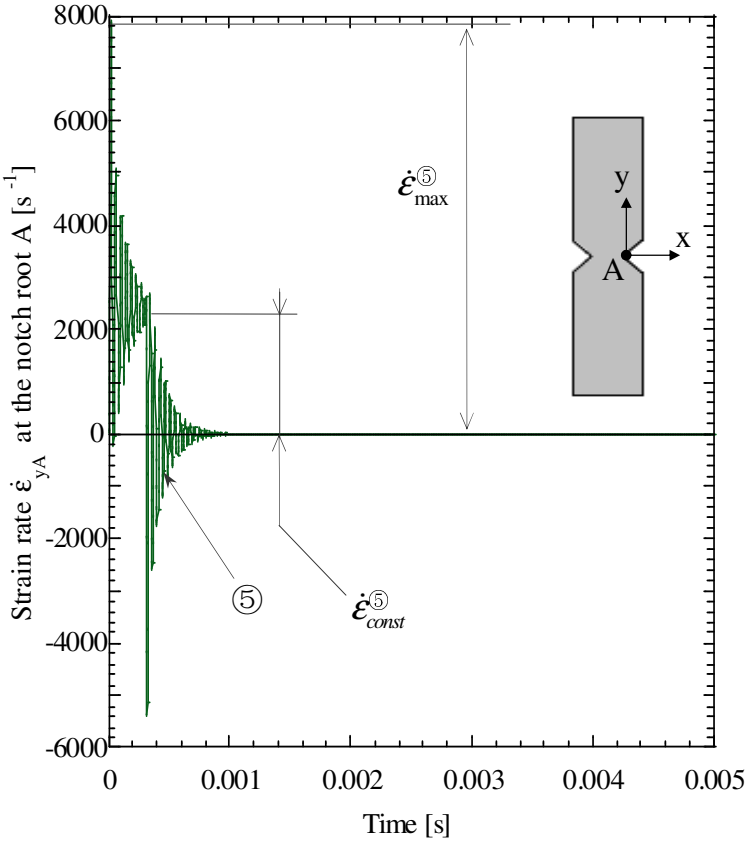

(e) Case 5

Figure 7. Strain rate at notch root A for ρ=0.03mm (Continued)

rate becomes constant. After stopping the forced displacement, several oscillations appear again, then it eventually converges to zero. From the comparison between Case 3 and Case 4, it is seen that the same maximum strain rate $\dot{\varepsilon}_{\max}$ and the same converged strain rate $\dot{\varepsilon}_{const}$ are observed although the final displacement $u_{\max}$ of Case 3 is 15 times larger than that in Case 2. It may be concluded that the strain rate concentration is controlled by the tensile speed. Figure 8 shows the

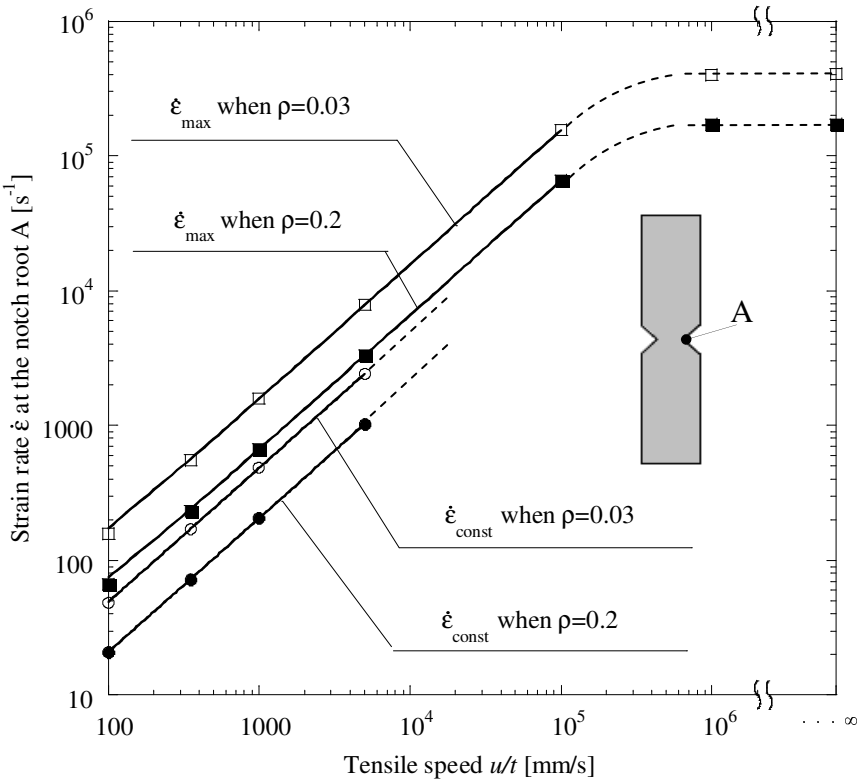

Figure 8. Maximum strain rate and converged strain rate vs. tensile speed

relationship between the tensile speed u/t and the strain rate for $\rho = 0.03mm$ and $0.2mm$. Here the results for $u/t = 10^5, 10^6\ mm/s$ and step load $u/t = \infty$ are also indicated when the maximum displacement is $1.5mm$. It is seen that the strain rate is proportional to the tensile speed when $u/t \le 5000\ mm/s$. However, the strain rate becomes constant when $u/t \ge 10^5\ mm/s$.

5. Dynamic stress and strain rate distributions of the minimum section

Figure 9(a) and Fig.10(a) show the dynamic stress distributions at the minimum section when the maximum dynamic stress appears. From Fig. 9(a), it is seen that the maximum dynamic stress $\sigma_{\max}(t)$ at the notch root when $\rho = 0.03mm$ is 14.48 times than that of the nominal stress $\sigma_{nom}(t)$ at the minimum section at each time for Case 1 –Case 5. On the other hand, from Fig. 10(a), it is seen that the maximum dynamic stress $\sigma_{\max}(t)$ at the notch root when $\rho = 0.2mm$ is 6.43 times than that of the nominal stress $\sigma_{nom}(t)$ at the minimum section at each time for Case 1 –Case 5. The stress concentration factor coincides with the static stress concentration factor obtained by Noda–Takase [12]. Figure 9(a) and Fig.10(a) show the strain rate distributions at the minimum section when the maximum strain rate appears. From Figure 9 (b), it is seen that the maximum strain rate $\dot{\varepsilon}_{\max}(t)$ at notch root when $\rho = 0.03mm$ is 22.87 times than that of the nominal strain rate $\dot{\varepsilon}_{nom}(t)$ at the minimum section for Case 1 –Case 5. From Fig. 10 (b), it is seen that the maximum strain rate $\dot{\varepsilon}_{\max}(t)$ at the notch root when $\rho = 0.2mm$ is 8.72 times than that of the nominal strain rate $\dot{\varepsilon}_{nom}(t)$ at the minimum section for Case 1 –Case 5.

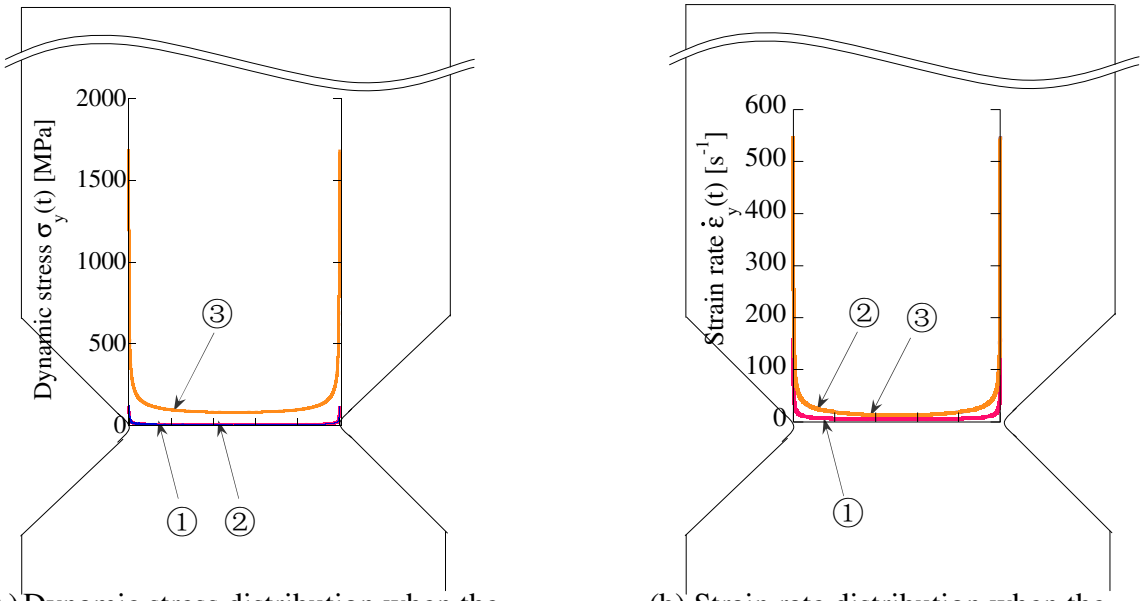

(A) Dynamic stress distribution when the maximum dynamic stress appeared

(b) Strain rate distribution when the maximum strain rate appeared

Figure 9. Stress and strain rate distribution around minimum section of ρ=0.03 mm

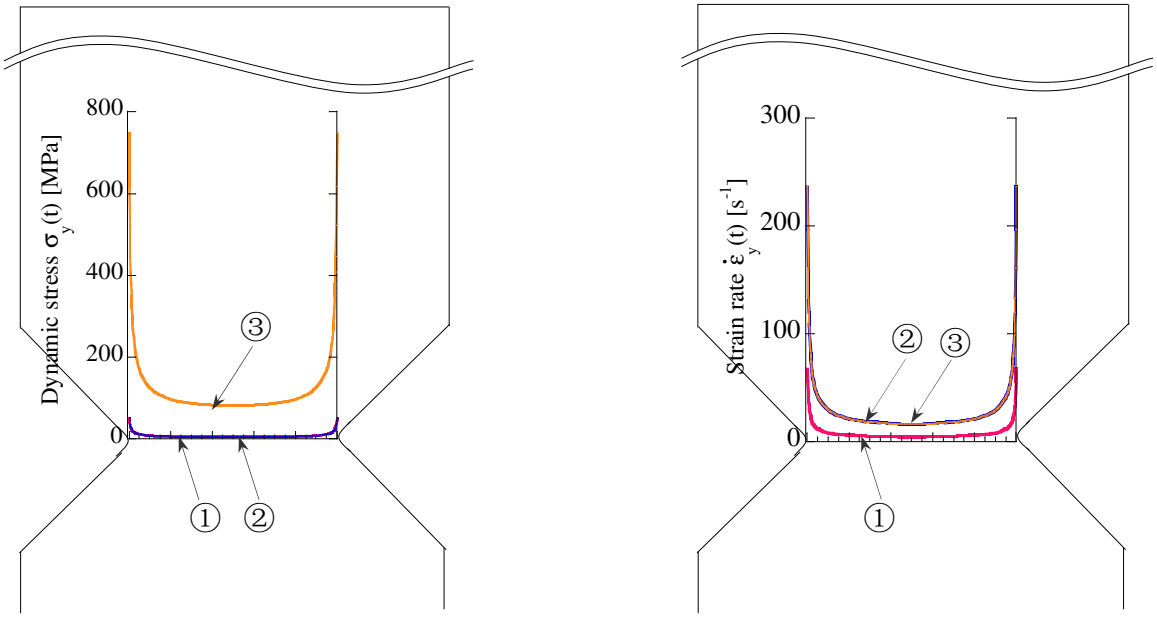

(A) Dynamic stress distribution when the maximum dynamic stress appeared

(b) Strain rate distribution when the maximum strain rate appeared

Figure 10. Stress and strain rate distribution around minimum section of ρ=0.2mm

6. Conclusion

Recently, high-speed tensile test is being used as a standard testing method to evaluate impact strength of the materials. For polymeric material, the strain rate and dynamic stress concentration is

significant factors, when we use this material as cellphone bumper. However, it is not easy to measure the dynamic stress or strain rate accurately at the notch root by experiment. In this study, therefore, dynamically and elastic FEM is applied to the high-speed tensile test for notched specimens. Then, the dynamic stress and strain rate concentrations have been discussed under various tensile speeds. The conclusions can be made the following way.

(1) It may be concluded that the strain rate concentration factor $K_{t\dot{\varepsilon}} = \dot{\varepsilon}_{\max}(t)/\dot{\varepsilon}_{nom}(t)$, which is defined by the maximum strain rate $\dot{\varepsilon}_{\max}(t)$ at the notch root over the average strain rate $\dot{\varepsilon}_{nom}(t)$ at the minimum section at each time, is always constant and controlled by the notch shape alone independent of the tensile speed.

(2) It is found that the difference between the static and dynamic maximum stress concentration ($\sigma_{\max} - \sigma_{st}$) at the notch root increases is proportional to the tensile speed when $u/t \le 5000\,mm/s$.

(3) It is found that the strain rate of the notch root increases is proportional to the tensile speed when $u/t \le 5000\,mm/s$.

References

[1] J. Radin, W. Goldsmith, Normal missile penetration and perforation of layered plates. Int. J. Impact Engng, 7, (1988) 229-259.

[2] T. Aya, T. Nakayama, Influence of Strain Rate on Elastic Modulus of Polymers. Journal of the Japan Society for Technology of Plasticity, Sosei-to-Kako, 36, 413 (1995) 665-670.

[3] S. Honma, Practical strength and durability of plastics (in Japanese). Plastics, 55, 1, (2004) 174-182.

[4] A. Chatani, S. Uchiyama, Dynamic stress concentration of notched strips. Material, 21, 226 (1972) 636-640.

[5] W. Altenhof, N. Zamani, W. North, B. Arnold, Dynamic stress concentrations for an axially loaded strut at discontinuities due to an elliptical hole or double circular notches. International Journal of Impact Engineering, 30, 3 (2004) 255-274.

[6] K. Kawata, S. Hashimoto, Dynamic stress concentration for notched elastic bar under dynamic load. University of Tokyo Institute of Space Aeronautical Report (in Japanese), 8, 2 (1972) 377-384.

[7] H. Matsumoto, I. Nakahara, Dynamic stresses in a hollow cylinder or a disc with a hole due to axially symmetric pressure variations. Transactions of the Japan Society of Mechanical Engineers, 32, 237 (1966) 709-717.

[8] H.G.. Georgiadis, A.P. Rigatos, N.C. Charalambakis, Dynamic stress concentration around a hole in a viscoelastic plate. Acta Mechanica, 111, 1-2 (1995) 1-12.

[9] S. Tanimura, Dynamic problems of materials and structures review of the studies. Transactions of the Japan Society of Mechanical Engineers, Series A, 63, 616 (1997) 2466-2471.

[10] N. Takeda, Impact damage and fracture of advanced composite materials/structures, Transactions of the Japan Society of Mechanical Engineers, Series A, 63, 616 (1997) 2472-2477.

[11] H. Inoue, K. Kishimoto, S. Aoki, Inverse analysis in impact problems. Transactions of the Japan Society of Mechanical Engineers, Series A, Vol. 63, No. 616 (1997), pp. 2478-2484.

[12] N.A. Noda, Y. Takase, Fatigue Notch Strength Useful for Machine Design (in Japanese), Nikkan Kogyo Shimbun Ltd, Tokyo, 2010.